HOSTED BY

Available online at www.sciencedirect.com
ScienceDirect
Journal of Radiation Research and Applied Sciences
journal homepage: http://www.elsevier.com/locate/jrras

Photoluminescence properties of europium doped di-strontium magnesium di-silicate phosphor by solid state reaction method

Ishwar Prasad Sahu [a,*], *D.P. Bisen* [a], *Nameeta Brahme* [a], *Raunak Kumar Tamrakar* [b]

[a] *School of Studies in Physics & Astrophysics, Pt. Ravishankar Shukla University, Raipur, CG 492010, India*
[b] *Department of Applied Physics, Bhilai Institute of Technology (Seth Balkrishan Memorial) Durg, CG 491001, India*

ARTICLE INFO

Article history:
Received 27 October 2014
Accepted 17 December 2014
Available online 30 December 2014

Keywords:
$Sr_2MgSi_2O_7:Eu^{3+}$
XRD
TEM
FTIR
Photoluminescence

ABSTRACT

Europium doped di-strontium magnesium di-silicate phosphor namely ($Sr_2MgSi_2O_7:Eu^{3+}$) was prepared by the traditional high temperature solid state reaction method. The phase structure of sintered phosphor was akermanite type structure which belongs to the tetragonal crystallography with space group $P\bar{4}2_1m$, this structure is a member of the melilite group and forms a layered compound. The EDX and FTIR spectra confirm the present elements in $Sr_2MgSi_2O_7:Eu^{3+}$ phosphor. Photoluminescence measurements showed that the phosphor exhibited strong emission peak with good intensity, corresponding to $^5D_0 \rightarrow {}^7F_2$ (613 nm) red emission and weak $^5D_0 \rightarrow {}^7F_1$ (590 nm) orange emission. The excitation spectra monitored at 613 nm show broad band from 220 to 300 nm ascribed to O–Eu charge-transfer band (CTB) centered at about 269 nm, and the other peaks in the range of 300–400 nm originated from f–f transitions of Eu^{3+} ions. The strongest band at 395 nm can be assigned to $^7F_0$ / $^5L_6$ transition of Eu^{3+} ions due to the typical f–f transitions within Eu^{3+} of $4f^6$ configuration.

1. Introduction

Light-emitting diodes (LEDs) have recently attracted attention as novel sources for illuminating light. LEDs have several advantages over fluorescent lights, including a longer operating life, better energy efficiency and a mercury-free composition (Schubert & Kim, 2005). Such LEDs, are in the early stages of development, and addressing the problem of their color rendering characteristics is particularly important. It is well known that white LEDs are mainly fabricated by combining blue LEDs with a yellow-emitting phosphor ($YAG:Ce^{3+}$). However, the white light obtained has a poor color rendering, because the yellow emission of $YAG:Ce^{3+}$ lacks any red and blue-green emissions (Hirosaki et al., 2005; Neeraj, Kijima, & Cheetham, 2004; Wu et al., 2005). Recently, one solution to this problem has been to fabricate a white LED with high color rendering by combining red, green and blue emitting tricolor phosphors with irradiation by a near UV LED. Therefore, the development of red and green phosphors show high emission intensities is desired (Kamei, Kojima, & Nishimiya, 2010).

* *Corresponding author*. Tel.: +91 9926993644.
E-mail address: ishwarprasad1986@gmail.com (I.P. Sahu).
Peer review under responsibility of The Egyptian Society of Radiation Sciences and Applications.
http://dx.doi.org/10.1016/j.jrras.2014.12.006

Melilites, which are generally formulated as $M_2T(1)T(2)_2O_7$ (where M and T(1) are usually the alkaline-earths or transition metals [M = Sr, Ca, Ba; and T(1) = Mg, Zn], and T(2)is usually Al, Ga, Si or Ge), have been investigated widely as optical materials [10]. Due to their tetragonal and non-centrosymmetric crystal structure, lanthanides or transition metals can be accepted easily as constituents or dopants by the melilites, allowing the synthesis of high-quality doped single crystals (Kaminskii et al., 2008). The silicate matrix $Sr_2MgSi_2O_7$ is a typical melilite. Phosphors based on this material are usually low-cost and are chemically and physically stable. They have been studied widely with Eu^{2+} doping, which shows that a blue emission and long persistent luminescence by co-doping with some other rare earth ions (Calson et al., 2009; Pan et al., 2008; Xu & Chen, 2008). Eu^{3+} ions were chosen as a luminescent species in many cases (Li, Guan, Li, Wen, & Yang, 2010; Nguyen, Mho, & Yeo, 2009; Srvastave, 2009; Volanti et al, 2009; Yang, Ren, Tao, Cui, & Yang, 2009) for the reasons of measurable lifetimes up to at least 1100 and simple luminescent spectra when compared to other rare earths (Chambers, Rousseve, & Clarke, 2009; Wan, Wang, Chen, Qian Li, & Mu, 2005). It is interesting to investigate the luminescent properties of Eu^{3+} in $Sr_2MgSi_2O_7$ matrix with the purpose of synthesis of a low cost and high efficiency orange – red phosphor.

In the present paper, we report the synthesis of europium doped di-strontium magnesium di-silicate ($Sr_2MgSi_2O_7$:Eu^{3+}) phosphor by high temperature solid state reaction method. This paper reports the structural characterization on the basis of XRD, TEM, FESEM, EDX and FTIR analysis and studies of optical properties are also done on the basis of photoluminescence (PL).

2. Experimental

2.1. Synthesis

Europium doped di-strontium magnesium di-silicate $Sr_2MgSi_2O_7$:Eu^{3+} phosphor was prepared by the high temperature solid state reaction method. The raw materials are strontium carbonate [$SrCO_3$ (99.90%)], magnesium oxide [MgO (99.90%)], silicon di-oxide [SiO_2 (99.99%)] and europium oxide [Eu_2O_3 (99.99%)], all of analytical grade (A.R.), were employed in this experiment. Boric acid (H_3BO_3) was added as flux. Initially, the raw materials were weighed according to the nominal compositions of $Sr_2MgSi_2O_7$:Eu^{3+} phosphor. Then the powders were mixed and milled thoroughly for 2 h using mortar and pestle. The grinded sample was placed in an alumina crucible and subsequently fired at 1200 °C for 3 h. At last the nominal compounds were obtained after the cooling down of programmable furnace.

2.2. Characterization techniques

The powder X-ray diffraction (XRD) pattern has been obtained by Bruker D8 advanced X-Ray powder diffractometer using CuKα radiation and the data were collected over the 2θ range 10–80°. Particle size of prepared $Sr_2MgSi_2O_7$:Eu^{3+} phosphor was determined by TEM using TECHNAI G2. The samples required for TEM analysis were prepared by dispersing the sintered phosphor in methanol using an ultrasound bath technique. A drop of this dispersed suspension was put onto 200-mesh carbon coated copper grid and then dried into the

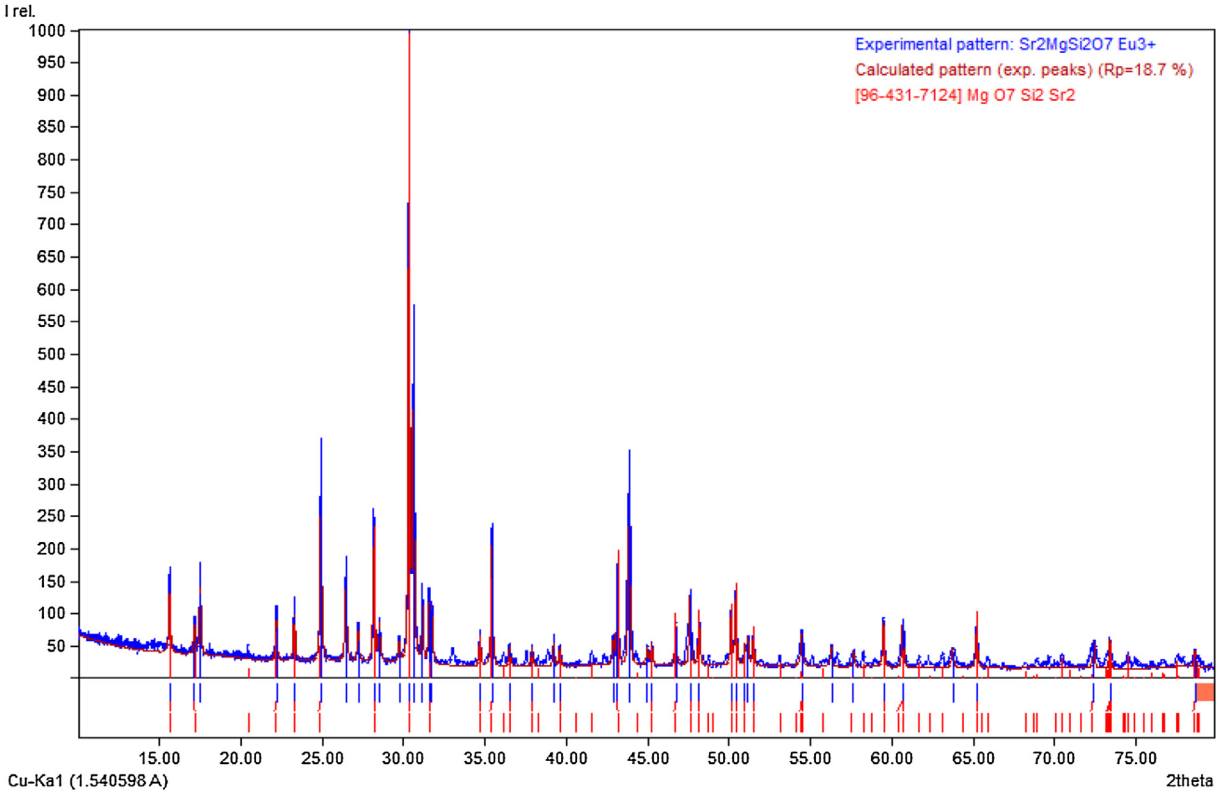

Fig. 1 – X-ray diffraction patterns of $Sr_2MgSi_2O_7$:Eu^{3+} phosphor.

air. The surface morphology of prepared $Sr_2MgSi_2O_7:Eu^{3+}$ phosphor was determined by the FESEM (ZIESS Ulta Plus-55) operated at the acceleration voltage of 5 kV. The samples were coated with a thin layer of gold (Au) and then surface morphology of prepared phosphor was observed. Energy dispersive spectroscopy (EDX) was used for the elemental (quantitative and qualitative) analysis of the prepared phosphor. FTIR spectra were recorded with the help of IR Prestige-21 by SHIMADZU for investigating the functional group region (4000–1400 cm^{-1}) as well as the finger print region (1400–400 cm^{-1}) of sintered phosphor in middle infrared region (4000–4000 cm^{-1}) by mixing the sample with potassium bromide (KBr, IR grade). The PL excitation and emission spectra were measured by a spectrofluorophotometer (SHIMADZU, RF-5301 PC). All measurements were carried out at the room temperature.

3. Results and discussions

3.1. XRD analysis

In order to determine the phase structure, powder XRD analysis has been carried out. The typical XRD patterns of $Sr_2MgSi_2O_7:Eu^{3+}$ phosphor with the standard XRD pattern is shown in Fig. 1. The position and intensity of diffraction peaks of the prepared $Sr_2MgSi_2O_7:Eu^{3+}$ phosphor were matched and found to be consistent with the standard XRD pattern (COD card No. 96-431-7124) by MATCH 2 software. The figure of merit (FOM) while matching these was 0.9671 (96%) which illustrates that the phase of the prepared sample agrees with the standard pattern COD card No. 96-431-7124. In Fig. 1, it can be concluded that prepared samples are chemically and structurally $Sr_2MgSi_2O_7$ phosphor. The crystalline phase of the prepared $Sr_2MgSi_2O_7:Eu^{3+}$ phosphor is nearly same ($a = b = 7.9948$ Å and $c = 5.1636$ Å) with the standard lattice parameters ($a = b = 7.9957$ Å and $c = 5.1521$ Å). The phase structure of the $Sr_2MgSi_2O_7:Eu^{3+}$ phosphor is akermanite type structure which belongs to the tetragonal crystallography with space group $P\overline{42}_1m$ (113 space number and D^3_{2d} space group), this structure is a member of the melilite group and forms a layered compound. The average crystallite size was calculated from the XRD pattern using Debye Scherrer relation $D = k\lambda/\beta\cos\theta$, where D is the crystallite size for the (hkl) plane, λ is the wavelength of the incident X-ray radiation [CuKα (0.154 nm)], β is the full width at half maximum (FWHM) in radiations, and θ is the corresponding angle of Bragg diffraction. Sharper and isolated diffraction peaks such as $2\theta = 30.48$ were chosen for calculation of the crystallite size. Based on the Debye-Scherrer's formula, the average crystallite size of $Sr_2MgSi_2O7:Eu^{3+}$ is ~67.

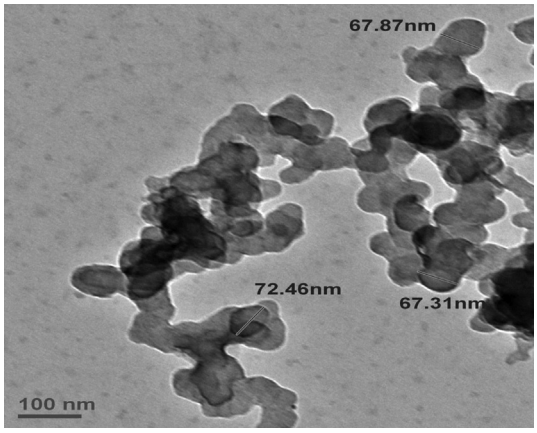

Fig. 2 – TEM image of $Sr_2MgSi_2O_7:Eu^{3+}$phosphor.

3.2. Transmission electron microscopy (TEM)

The particle size of $Sr_2MgSi_2O_7:Eu^{3+}$ is shown in Fig. 2. The TEM images confirm the particle size of the prepared phosphor. From the TEM image, it can be observed that the prepared sample consists of grain with different size distribution. Moreover, the agglomeration of powder particles was also observed due to high temperature. The transmission electron microscopy results are in good correlation with the XRD result.

3.3. Field emission scanning electron microscopy (FESEM)

The surface morphology of the $Sr_2MgSi_2O_7:Eu^{3+}$ phosphor is shown in Fig. 3(a,b) with different magnification. The surface morphology of the particles was not uniform and they aggregated tightly with each other due to the high temperature heat treatment. Moreover, the agglomeration of powder particles was also observed. From the FESEM image, it can be observed that the prepared sample consists of particles with different size distribution. The scanning electron microscopy results are in good correlation with the TEM result.

3.4. Energy dispersive X-Ray spectroscopy (EDX)

The composition of the powder sample has been measured using EDX. Energy dispersive x-ray spectroscopy (EDX) is a standard procedure for identifying and quantifying elemental composition of sample area as small as a few nanometers.

The existence of europium (Eu) in prepared phosphor is clear in their corresponding EDX spectra. Their appeared no other emission apart from strontium (Sr), magnesium (Mg), silicon (Si) and oxygen (O) in $Sr_2MgSi_2O_7:Eu^{3+}$ EDX spectra of the samples. In the EDX spectrum, the presence of Sr, Mg, Si, O and Eu, intense peak are present which preliminary indicates the formation of $Sr_2MgSi_2O_7:Eu^{3+}$ phosphor in Fig. 4.

3.5. Fourier transform infrared spectra (FTIR)

The Fourier Transform Infrared (FTIR) spectra have been widely used for the identification of organic and inorganic compounds. Fig. 5 shows the FTIR spectra of $Sr_2MgSi_2O_7:Eu^{3+}$ phosphor. In observed IR spectrum, the absorption bands of silicate groups are clearly evident. An intense band centred at 974.14 cm^{-1} is assigned due to Si–O–Si asymmetric stretch, bands at 874.98 and 631.89 cm^{-1} to Si–O symmetric stretch. Bands at 513.54 and 467.17 cm^{-1} are assigned to Si–O–Si vibrational mode of bending. Furthermore, in keeping with the absorption bands, posited at 1089.29, 924.56 778.62, 716.65

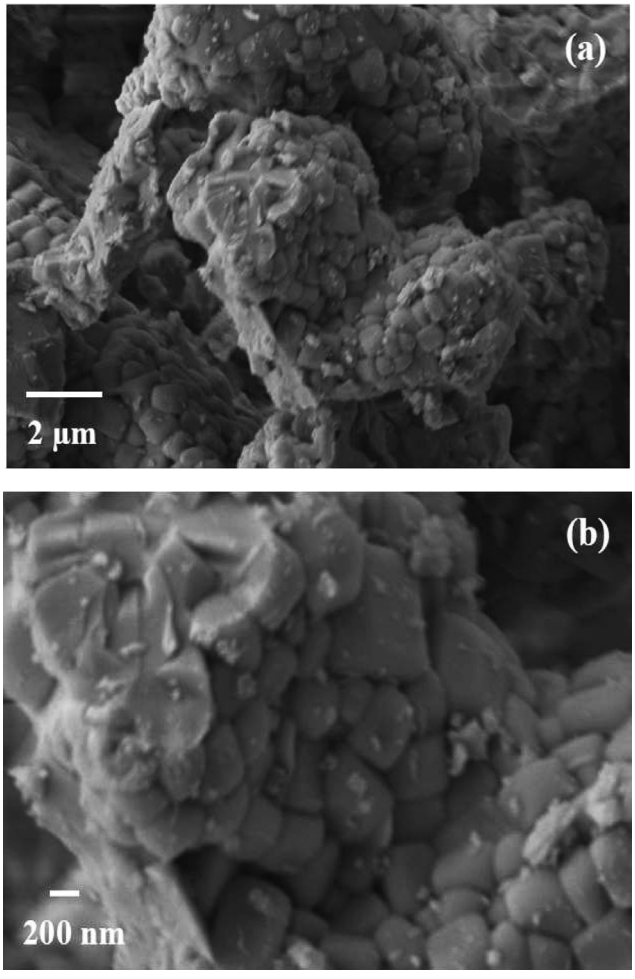

Fig. 3 – (a, b) FESEM image of $Sr_2MgSi_2O_7$: Eu^{3+} phosphor.

and 667.08 cm^{-1} respectively can be ascribed to the presence of SiO_4 group (Gou, Chang, & Zhai, 2005).

The FTIR spectrum of $Sr_2MgSi_2O_7$:Eu^{3+} phosphor contains clearly exhibited bands in the region (3421.05 cm^{-1}) of hydroxyl group show the stretching vibration of O–H groups. The hydroxyl group in sintered phosphor is might be due to presence of moisture through environment. The asymmetric stretching of (CO_3^{2-}) carbonates can be observed in the range of 1900–1700 cm^{-1}. Two weak shoulders, which corresponds to the out of plane bending of appears at approximately 1980.58,

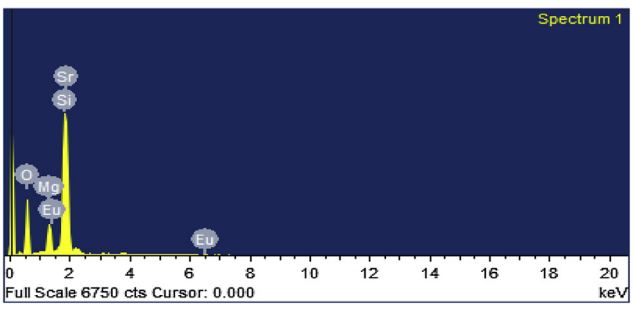

Fig. 4 – EDX spectra of $Sr_2MgSi_2O_7$:Eu^{3+} phosphor.

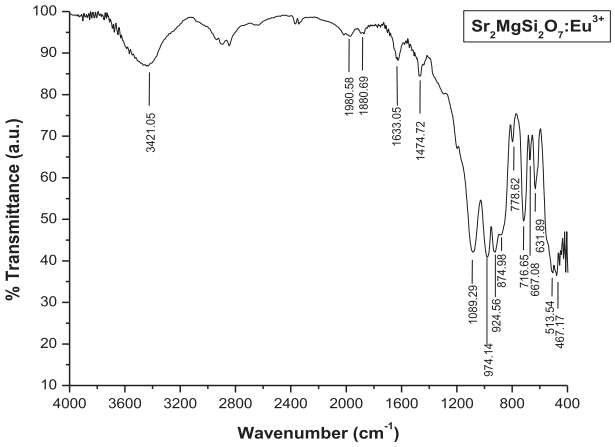

Fig. 5 – FTIR Spectra of $Sr_2MgSi_2O_7$:Eu^{3+} phosphor.

1880.69 cm^{-1}. These bands are due to a slight carbonation of the samples preparation [$SrCO_3$ (raw material)]. The free CO_3^{2-} ions has a D3h symmetry (trigonal planar) and its spectrum is dominated by the band at 1900–1700 cm^{-1}. The vibration band of 1633.05 cm^{-1} are assigned due to the Mg^{2+} and bending of the sharp peaks in the region of 1474.72 cm^{-1} are assigned due to Sr^{2+}. When Eu^{3+} enters the lattice, it will replace the Sr^{2+} in the $Sr_2MgSi_2O_7$ host and occupy Sr^{2+} lattice sites due to distortion in the $Sr_2MgSi_2O_7$ host crystal lattice. Original position of Sr^{2+} was replaced by Eu^{3+} and the original of Sr^{2+} located at somewhere (Sahu, Bisen, & Brahme, 2014a, 2014b, 2014c). Therefore the vibration mode of Sr^{2+} at 1474.72 cm^{-1} is clearly observed from $Sr_2MgSi_2O_7$:Eu^{3+} phosphor. Another fact that supports that the radius of Eu^{3+} (1.07 Å) are very close to that of Sr^{2+} (about 1.12 Å) rather than Mg^{2+} (0.65 Å) and Si^{4+} (0.41 Å). Therefore, the Eu^{3+} ions are expected to occupy the Sr^{2+} sites in the $Sr_2MgSi_2O_7$:Eu^{3+} phosphor (Chandrappa, Ghosh, & Patil, 1999; Fei, Chang, & Mao, 2005; Salim et al., 2009).

3.6. *Photoluminescence (PL)*

Fig. 6 shows the PL spectrum of $Sr_2MgSi_2O_7$:Eu^{3+} phosphor. The sintered phosphor would excited by 395 nm. As shown in Fig. 1, the emission spectrum is mainly composed of two strong emission peaks. The emission spectrum exhibits four typical emission peaks in the range of 560–700 nm, which result from $^5D_0 \rightarrow {}^7F_j$ (J = 0, 1, 2, 3 and 4). The emission peak at 613 nm is ascribed to the electric dipole transition from $^5D_0 \rightarrow {}^7F_2$ of Eu^{3+}, while the emission near 593 nm is assigned to the magnetic dipole transition from the $^5D_0 \rightarrow {}^7F_1$ of Eu^{3+}. Moreover, there are two weak emission peaks located at 580 and 652 nm, which are ascribed to $^5D_0 \rightarrow {}^7F_0$ and $^5D_0 \rightarrow {}^7F_3$ transitions of Eu^{3+} respectively.

According to the parity selection rule, when the Eu^{3+} ions are located at the site with an inversion symmetric center, the $^5D_0 \rightarrow {}^7F_1$ magnetic dipole transition is permitted, which results in orange red emitting around 590 nm. But if located at the site without an inversion symmetric center, because the opposite parity 5d configuration is mixed into $4f^n$

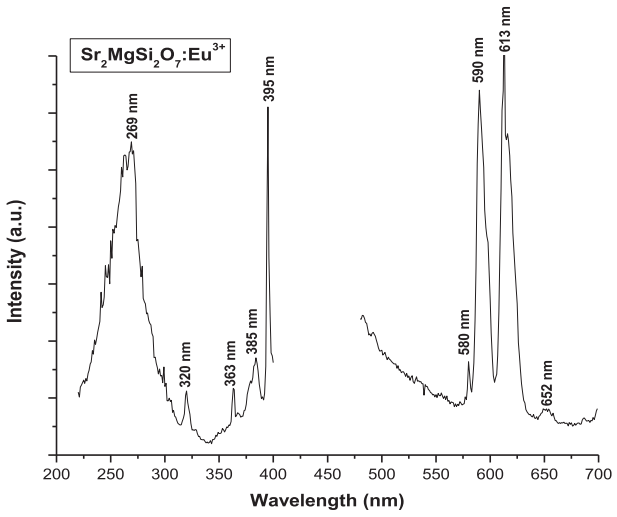

Fig. 6 – Photoluminescence Spectra of $Sr_2MgSi_2O_7:Eu^{3+}$ phosphor.

configuration, the parity selection rule is able to be lifted, and f–f forbidden transition is partially released, the hypersensitive $^5D_0 \rightarrow {}^7F_2$ electric dipole transition will be permitted, which results in red emitting around 613 nm. For the phosphor $Sr_2MgSi_2O_7:Eu^{3+}$ prepared in our experiment, the strongest red emission peak is located at 613 nm will be dominated. It can be presumed that Eu^{3+} ions mainly occupy non-inversion symmetric center in host lattice (Sun, Qian, Liao, Wang, & Yan, 2001).

3.7. *CIE chromaticity coordinate*

In general, color of any phosphor material is represented by means of color coordinates. The luminescence color of the samples excited under 395 nm has been characterized by the CIE (Commission International de I'Eclairage) 1931 chromaticity diagram. The emission spectrum of the Eu^{3+} doped $Sr_2MgSi_2O_7$ phosphor was converted to the CIE, 1931 chromaticity using the photoluminescent data and the interactive CIE software (CIE coordinate calculator) diagram as shown in Fig. 7. Every natural color can be identified by (x, y) coordinates that are disposed inside the 'chromatic shoe' representing the saturated colors (Sahu et al., 2014a, 2014b, 2014c). Luminescence colors of Eu^{3+} doped $Sr_2MgSi_2O_7$ phosphor are placed in the orange–red (X = 0.5497, Y = 0.4447) corners. The chromatic co-ordinates of the luminescence of this phosphor are measure and reached to orange–red luminescence.

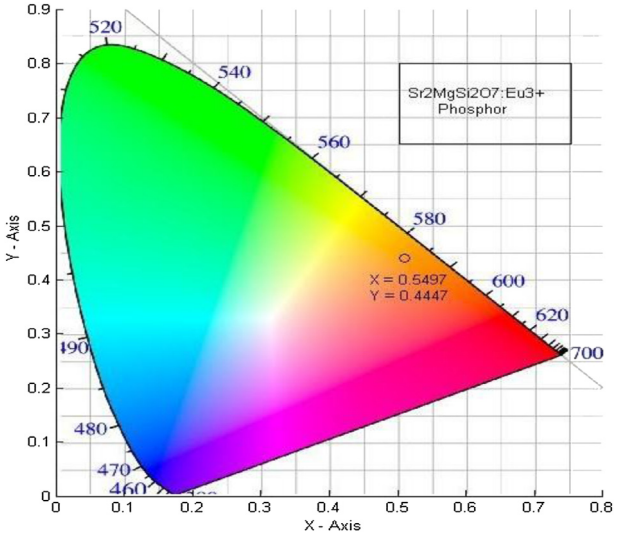

Fig. 7 – CIE diagram of $Sr_2MgSi_2O_7:Eu^{3+}$ phosphor.

4. Conclusion

In summary, we have successfully synthesized pure tetragonal phased $Sr_2MgSi_2O_7:Eu^{3+}$ phosphor via traditional high temperature solid state reaction method. The phase structure of the $Sr_2MgSi_2O_7:Eu^{3+}$ phosphor is consistent with standard tetragonal crystallography. From the XRD and TEM analysis, average particle size of $Sr_2MgSi_2O_7:Eu^{3+}$ phosphor was ~67 nm. The radius of Eu^{3+} (1.07 Å) are very close to that of Sr^{2+} (about 1.12 Å) rather than Mg^{2+} (0.65 Å) and Si^{4+} (0.41 Å). Therefore, the Eu^{3+} ions are expected to occupy the Sr^{2+} sites in the $Sr_2MgSi_2O_7:Eu^{3+}$ phosphor. The EDX and FTIR spectra confirm the present elements in $Sr_2MgSi_2O_7:Eu^{3+}$ phosphor. Under the near ultraviolet (NUV) excitation (395 nm), photoluminescence measurements showed that the phosphor exhibited strong emission peak with good intensity corresponding to $^5D_0 \rightarrow {}^7F_2$ (613 nm) red emission and weak $^5D_0 \rightarrow {}^7F_1$ (590 nm) orange emission. The PL emission exhibited orange–red light which was confirmed from the calculated CIE coordinates. Thus, the solid state reaction method furnishes a simple method for preparing a silicate based phosphor.

Acknowledgments

"We are very grateful to UGC-DAE Consortium for Scientific Research, Indore (M.P.) for the XRD Characterization and we are very thankful Dr. Mukul Gupta for his co-operation". We are very much thankful to Dr. K.V.R. Murthy, Department of Applied Physics, M.S. University Baroda, Vadodara (Gujarat) India for the photoluminescence study.

REFERENCES

Carlson, S., Holsa, J., Laamanen, T., Latsusaari, M., Malkamaki, M., & Niittykoski, J. (2009). X-ray absorption study of rare earth ions in $Sr_2MgSi_2O_7:Eu^{2+}$, R^{3+} persistent luminescence materials. *Optical Materials, 31*, 1877–1879.

Chambers, M. D., Rousseve, P. A., & Clarke, D. R. (2009). Decay pathway and high-temperature luminescence of Eu^{3+} in $Ca_2Gd_8Si_6O_{26}$. *Journal of Luminescence, 129*, 263–269.

Chandrappa, G. T., Ghosh, S., & Patil, K. C. (1999). Synthesis and properties of willemite, Zn_2SiO_4, and $M^{2+}:Zn_2SiO_4$ (M = Co and Ni). *Journal of Materials Synthesis and Processing, 7*, 273–279.

CIE. (1971). *International commission on illumination*. Publication CIE no. 15 (E-1.3.1).

Fei, Q., Chang, C., & Mao, D. (2005). Luminescent properties of $Sr_2MgSi_2O_7$ and $Ca_2MgSi_2O_7$ long lasting phosphors activated by Eu^{2+}, Dy^{3+}. *Journal of Alloys and Compounds, 390*(1–2), 133–137.

Gou, Z., Chang, J., & Zhai, W. (2005). Preparation and characterization of novel bioactive dicalcium silicate ceramics. *Journal of the European Ceramic Society, 25*, 1507–1514.

Hirosaki, N., Xie, R. J., Kimoto, K., Sekiguchi, T., Yamamoto, Y., Suehiro, T., et al. (2005). Characterization and properties of green-emitting β-SiAlON:Eu^2+ powder phosphors for white light-emitting diodes. *Applied Physics Letters, 86*, 211905.

Kamei, S., Kojima, Y., & Nishimiya, N. (2010). Preparation and fluorescence properties of novel red-emitting Eu^{3+} activated amorphous alkaline earth silicate phosphors. *Journal of Luminescence, 130*, 2247–2250.

Kaminskii, A. A., Bohaty, L., Becker, P., Liebertz, J., Held, P., & Eichler, H. J. (2008). Tetragonal $Ba_2MgGe_2O_7$ – a novel multifunctional optical crystal with numerous manifestations of nonlinear laser effects: almost sesqui-octave Stokes and anti-Stokes combs and cascaded $\chi^{(3)} \rightarrow \chi^{(2)}$ lasing with involved second and third harmonic generation. *Laser Physics Letters, 5*, 845–868.

Li, X., Guan, L., Li, X., Wen, J., & Yang, Z. (2010). Luminescent properties of $NaBaPO_4$:Eu^{3+} red-emitting phosphor for white light-emitting diodes. *Powder Technology, 200*, 12–15.

Neeraj, S., Kijima, N., & Cheetham, A. K. (2004). Novel red phosphors for solid state lighting: the system $NaM(WO_4)_{2-x}(MoO_4)_x$:Eu^{3+} (M = Gd, Y, Bi). *Chemical Physics Letters, 387*, 2–6.

Nguyen, H. D., Mho, I., & Yeo, I. H. (2009). Preparation and characterization of nanosized (Y,Bi)VO_4:Eu^{3+} and Y(V,P)O_4:Eu^{3+} red phosphors. *Journal of Luminescence, 129*, 1754–1758.

Pan, W., Ning, G., Zhang, X., Wang, J., Lin, Y., & Ye, J. (2008). Enhanced luminescent properties of long-persistent $Sr_2MgSi_2O_7$:Eu^{2+}, Dy^{3+} phosphor prepared by the co-precipitation method. *Journal of Luminescence, 128*, 1975–1979.

Sahu, I. P., Bisen, D. P., & Brahme, N. (2014a). Dysprosium doped di-strontium magnesium di-silicate White light emitting phosphor by solid state reaction method. *Displays, 35*, 279–286.

Sahu, I. P., Bisen, D. P., & Brahme, N. (2014b). Structural characterization and optical properties of $Ca_2MgSi_2O_7$:Eu^{2+} Dy^{3+}phosphor by solid-state reaction method. *Luminescence: The Journal of Biological and Chemical Luminescence*. http://dx.doi.org/10.1002/bio.2771. wileyonlinelibrary.com.

Sahu, I. P., Bisen, D. P., & Brahme, N. (2014c). Luminescence properties of Eu^{2+} and Dy^{3+} doped $Sr_2MgSi_2O_7$ and $Ca_2MgSi_2O_7$ phosphors by solid state reaction method. *Research on Chemical Intermediates*. http://dx.doi.org/10.1007/s11164-014-1767-6.

Salim, M. A., Hussain, R., Abdullah, M. S., Abdullah, S., Alias, N. S., & Ahmad Fuzi, S. A. (2009). The local structure of phosphor material, $Sr_2MgSi_2O_7$ and $Sr_2MgSi_2O_7$:Eu^{2+} by infrared spectroscopy. *Solid State Science & Technology, 17*, 59–64.

Schubert, E. F., & Kim, J. K. (2005). Solid-state light sources getting smart. *Science, 308*(5726), 1274–1278.

Srivastave, A. M. (2009). Chemical bonding and crystal field splitting of the Eu^{3+7} F_1 level in the pyrochlores $Ln_2B_2O_7$ (Ln = La^{3+}, Gd^{3+}, Y^{3+}, Lu^{3+}; B = Sn^{4+}, Ti^{4+}. *Optical Materials, 31*(6), 881–885.

Sun, L. D., Qian, C., Liao, C. S., Wang, X. L., & Yan, C. H. (2001). Luminescent properties of Li^+ doped nanosized Y_2O_3:Eu. *Solid State Communications, 119*(6), 393.

Volanti, D. P., Rosa, I. L. V., Paris, E. C., Paskocimas, C. A., Pizani, P. S., & Varela, J. A. (2009). The role of the Eu^{3+} ions in structure and photoluminescence properties of $SrBi_2Nb_2O_9$ powders. *Optical Materials, 31*, 995–999.

Wan, J., Wang, Z., Chen, X., Qian, L., & Mu, Y. (2005). Euro shape-induced enhanced luminescent properties of red phosphors: $Sr_2MgSi_2O_7$:Eu^{3+} Nanotubes. *European Journal of Inorganic Chemistry*, 4031–4034.

Wu, H., Zhang, X., Gao, C., Xu, J., Wu, M., & Su, Q. (2005). Three bands White light from InGaN-based LED Chip Precoated with Green/Red phosphors. *IEEE Xplore: Photonics Technology Letters, 17*, 1160.

Xu, Y., & Chen, D. (2008). Combustion synthesis and photoluminescence of $Sr_2MgSi_2O_7$:Eu,Dy long lasting phosphor nanoparticles. *Ceramics International, 34*(8), 2117–2120.

Yang, Y., Ren, Z., Tao, Y., Cui, Y., & Yang, H. (2009). Eu^{3+} emission in $SrAl_2B_2O_7$ based phosphors. *Current Applied Physics, 9*, 618–621.